GRIP: A GENERIC DATA REDUCTION PACKAGE FOR NULLING INTERFEROMETRY

Marc-Antoine Martinod[a,1], Denis Defrère[a], Romain Laugier[a], Steve Ertel[b,c], Olivier Absil[d], Barnaby Norris[e], Bertrand Mennesson[f].

[a]Institute of Astronomy, KU Leuven, Celestijnenlaan 200D, 3001 Leuven, Belgium; [b]Department of Astronomy and Steward Observatory, 933 North Cherry Ave, Tucson, AZ 89 85721, USA; [c]Large Binocular Telescope Observatory, 933 North Cherry Ave, Tucson, AZ 85721, USA; [d]Space sciences, Technologies & Astrophysics Research (STAR) Institute, University of Liège, Liège, Belgium; [e]Sydney Institute for Astronomy, School of Physics, Physics Road, University of Sydney, NSW 2006, Australia; [f]Jet Propulsion Laboratory, California Institute of Technology (United States).

ABSTRACT

Nulling interferometry is a powerful observing technique to study exoplanets and circumstellar dust at separations too small for direct imaging with single-dish telescopes. With recent photonics developments and the near-future ground-based instrumental projects, it bears the potential to detect young giant planets near the snow lines of their host stars. The observable quantity of a nulling interferometer is called the null depth, its precise measurement and calibration remain challenging against instrument and atmospheric noise. Null self-calibration is a method aiming to model the statistical distribution of the nulled signal. It has proven to be more sensitive and accurate than average-based data reduction methods in nulling interferometry. The variety of existing and upcoming of nullers raises the issue of consistency of the calibration process, structure of the data and the ability to reduce archived data on the long term. It has also led to many different implementations of the Null self-calibration method. In this article, we introduce `GRIP`: the first open-source toolbox to reduce nulling data with enhanced statistical self-calibration methods from any nulling interferometric instrument within a single and consistent framework. Astrophysical results show good consistency with two published GLINT and LBTI datasets and confirm nulling precision down to a few 10^{-4}.

Keywords Data Methods, Software, signal processing, high contrast imaging, high angular resolution, optimisation, model fitting, universal, self-calibration, statistical analysis

1 Introduction

Nulling interferometry is a powerful technique to perform high-contrast imaging in the close neighbourhood of the stars Bracewell [1978]. Pioneered on the Multiple-Mirror Telescope (MMT) in 1998 Hinz et al. [1998], it has been used over the past decades to detect and characterize habitable-zone dust around nearby stars. Similarly to the coronagraphy technique in direct imaging, nulling interferometry suppresses the on-axis source (e.g. a star) but proceeds differently : beams from two apertures are coherently combined to create a destructive

[1]mam.astro01@gmail.com

interference for on-axis sources. The offset in the optical path lengths induced by an off-axis sources (e.g. an exoplanet) is transmitted by the instrument, allowing a direct detection and characterisation of the object. The nulled depth N is linked to the modulus of the observed target's spatial coherence (also known as the visibility) V with $N = \frac{1-V}{1+V}$. Performing nulling requires extremely stable interferences to efficiently discriminate the photons coming from the planets from the ones coming from the starlight. The fainter the off-axis source, the better the stabilisation must be, to efficiently remove the starlight from the measured signal. Such observation is challenged by atmospheric turbulence and vibrations in the instrument and telescope.

Legacy data reduction techniques relied on measuring the average value of the null depth on the science and calibrator targets then performed a subtraction between the two to obtain the astrophysical null depth, solely governed by the object's geometry. The state-of-the-art method, to process nulling data sets, is the nulling self-calibration (NSC) Hanot et al. [2011]: it models the statistical fluctuations to provide a self-calibrated astrophysical null depth. In other words, this method directly measures the astrophysical null depth by fitting out null biases related to the instrumental response of the nulling interferometer. Therefore, the measurement is more precise and the observation of a reference star to measure this response is ideally not required.

The null self-calibration is a simulation-based inference method Cranmer et al. [2020]. Monte-Carlo simulations are carried out to reproduce the measured distributions. The model takes for parameters the distributions of the instrumental errors and the astrophysical null depth. The outcome is a sequence of simulated nulled flux. These data are sorted into a histogram, which is then compared with the histogram of the observed data through the optimization of a simple cost function. This process enables the self-calibration, provided that the simulator can correctly model the dominant effects of the instrument response. In some cases, calibration with reference targets is still required to remove sources of null errors that have not been simulated. One of the parameters is the astrophysical null depth, i.e. the observable which only depends on the surface brightness and the geometry of the target, free from the bias of the instrument response. The use of this technique on the Palomar Fiber Nuller yielded an improvement on the precision by a factor of 10 Hanot et al. [2011], Mennesson et al. [2011], Serabyn et al. [2019]. This method is now used on active nullers such as the Large Binocular Telescope Interferometer (LBTI) Defrère et al. [2016], Mennesson et al. [2016] and Guided-Light Interferometric Nulling Technology (GLINT) Norris et al. [2020], Martinod et al. [2021], yet through different implementations given the constraints from the instrument designs and how well characterised they were (e.g. grid search for the LBTI, least squares estimation for GLINT). It has enabled several scientific achievements on spectroscopic binaries Serabyn et al. [2019], exozodiacal dust Defrère et al. [2015, 2021], Ertel et al. [2018, 2020] and stellar diameters Martinod et al. [2021].

By relying on a Monte-Carlo approach and a clearly defined instrumental function, this technique can be used on any nuller. It shifts, for the first time, the way of doing data reduction in interferometry from a tailor-made pipeline for each instrument to a generic one providing self-calibrated measurements. This paper introduces the *Generic data reduction for nulling interferometry package* (GRIPMartinod et al. [2024]), the first project which aims to provide a collection of functions to reduce data from all existing (e.g. GLINT Martinod et al. [2021] or LBTI Defrère et al. [2016]) and future nulling instruments (e.g. Asgard/NOTT Defrère et al. [2018a] and the LIFE space mission Quanz et al. [2018, 2022]) in a consistent framework. This work is performed within the framework of the Asgard/NOTT project Defrère et al. [2018a,b, 2022], a future nulling interferometer under construction for the visitor focus of the VLTI .

2 Concept and workflow of GRIP

Having several nullers in different places of the world that observe at different wavelengths and rely on different architectures is an advantage to grasp a detailed knowledge of a given target. However, this represents a challenge for the consistency of the calibration process, different for each instrument, the structure of the data and the capability to reduce archived data in the future. A data reduction pipeline built upon the NSC technique tackles these challenges as it provides a unique, consistent, easy to maintain and universal way to reduce data from any kind of nuller. For instance, the `Vortex Imaging Processing` package Gomez Gonzalez et al.

[2017], Christiaens et al. [2023a] provides a collection of image processing routines that can be used to create pipelines to reduce direct imaging data Christiaens et al. [2023b, 2024].

GRIP is the first project in nulling interferometry providing a unique and consistent framework to provide self-calibrated null depth measurements. This toolbox offers several battle-tested optimisation strategies and cost functions to achieve this task. GRIP is a package designed to build a data reduction pipeline; it does not come as a stand-alone software.

Figure 1 details the inputs, outputs and features of GRIP to perform self-calibration. In the inputs, the user has to provide a simulator of the instrument (also called *simulator*), preprocessed data to extract the astrophysical null depth and ancillary data to be used by the simulator. The preprocessed data consists of sequences such as the flux or counts of outputs. Ancillary data are non-nulled data (e.g. photometries of the beams) and noise measurements (e.g. detector noise, thermal background, phase fluctuations...) needed to simulate the nulled signal. GRIP provides tools to turn these sequences of nulled and ancillary data into histograms. With the instrument model, it enables the generation of sequences of values of the same kind as the preprocessed data. These simulated sequences will then be turned into histograms. GRIP's features (such as optimisation strategies and cost functions) enable the processing of the histograms from the preprocessed and simulated data to deliver the self-calibrated quantities and the other fitted parameters. The workflow of GRIP (Fig. 2) follows these steps:

1. The user provides the instrument response function and identifies the free parameters to be fitted.
2. The measured null depth data (from the preprocessed data) and the measured ancillary are turned into histograms with GRIP;
3. The measured histograms of the ancillary data are used as probability density distributions to simulate their corresponding instrumental/atmospheric noises with the model;
4. Random sequences generated from the empirical distributions from the previous step are injected into the instrument simulator (provided by the user) to simulate nulled signal;
5. The simulated sequence is turned into histograms with GRIP;
6. The two histograms are used to calculate a cost function;
7. The cost function is minimized in a fitting algorithm (e.g. Levenberg Marquardt, MCMC, or other) until convergence by repeating the last 3 steps. The values of the free parameters at the convergence are the self-calibrated quantities.

3 Package overview

The code is being developed in Python, under the MIT license, and it is published on Github[2]. Its dependencies are widely-used Python packages such as NumPy and scipy. GRIP is a function-based package to give flexibility to the users to implement it into their pipeline. The documentation is made of description of the functions and tutorials, explaining the use of the features of the package. Particularly, one tutorial is provided to help the design of an instrument simulator to use with GRIP. GRIP runs on a GPU with the use of Cupy Okuta et al. [2017] or on CPU if this package is not installed when the package is used.

GRIP's features can be used to build a data reduction pipeline. These features are set in several modules (Table 1). A Monte-Carlo process is used to generate a sequence of data, turned into a histogram, which is fit to the observed histogram using optimisers from well-known third-party Python packages. The user defines the quantities to be generated during the Monte Carlo process and GRIP can efficiently reproduce any arbitrary distribution, allowing the use of the distributions of measured data.

GRIP is made of several modules, providing all the tools to make histograms, perform self-calibration measurements, visualise the results and check the goodness of the fit. The fitting and histogram_tools are

[2] https://github.com/mamartinod/grip

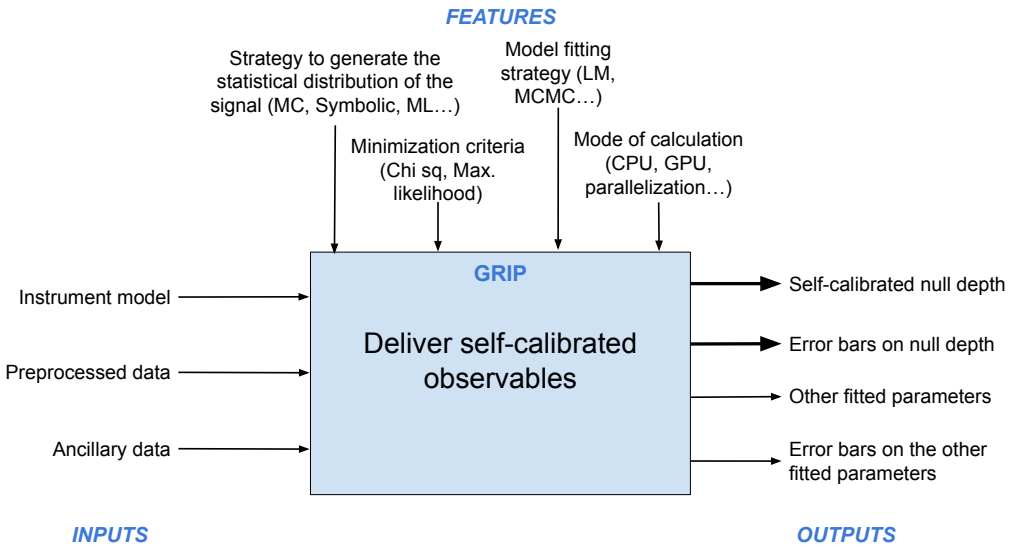

Figure 1: Structured analysis and design technique of GRIP. The left part lists the elements provided by the user and the right parts are the outputs of GRIP. The upper side lists the features of GRIP to process the data.

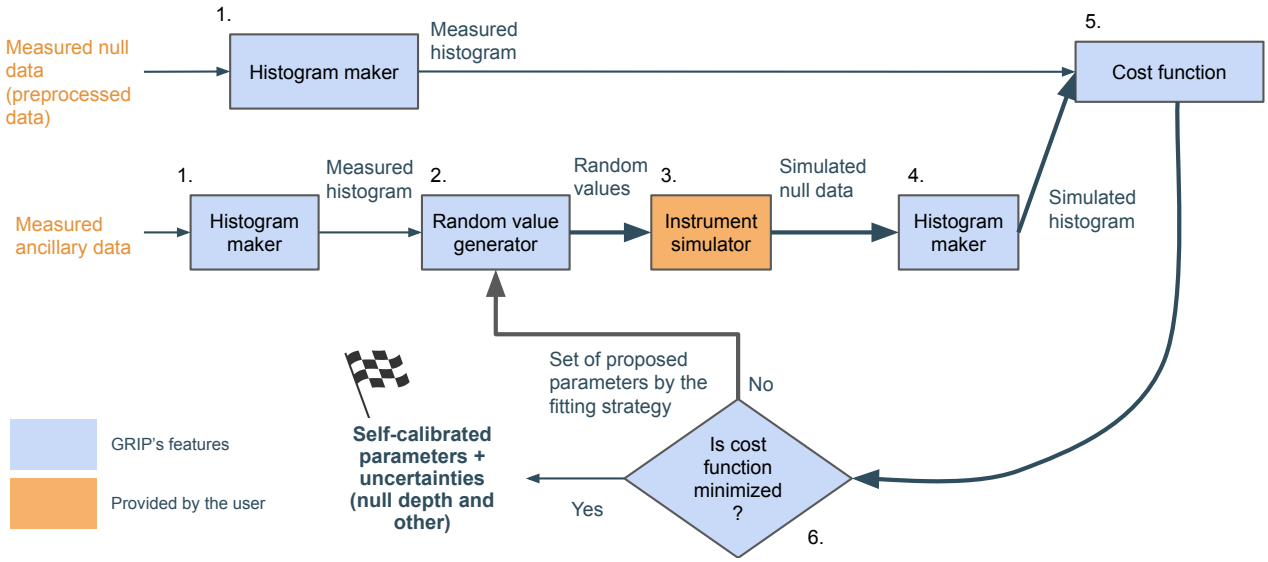

Figure 2: Workflow of GRIP. The blue boxes are GRIP's features and the blue text represents items generated by them. The orange box and text represents elements brought by the user.

Table 1: Modules of GRIP

`fitting`	Fitting optimisers, estimators for fitting and a parameter grid search
`generic`	Miscellaneous functions
`histogram_tools`	Histograms makers and random values generators
`instrument_models`	Instrument models such as GLINT Martinod et al. [2021] or LBTI Defrère et al. [2016]
`load_files`	Load HDF5 and FITS files
`plots`	Plot results of GRIP
`preprocessing`	Features such as sorting and data binning

core modules of `GRIP`. They contain all the utilities to perform null self-calibration (optimiser, cost function, random value generator, histogram maker) and can handle user-defined instrument simulators. The current optimisers available in GRIP are:

- `scipy.optimize.least_squares` with the dogbox method (least squares method);
- `scipy.optimize.minimize` with the Powell method (maximum likelihood estimator, or MLE);
- MCMC powered with the `emcee` package Foreman-Mackey et al. [2013] (Bayesian inference method). The used sampler is a mixture of `StretchMove` and `WalkMove` with the respective relative weight 0.2 and 0.8. This mixture minimizes the autocorrelation time compared to the use of a single sampler.

All methods accept bounded parameter space. The user can define these bounds with the help of the search grid to spot the optimal region to investigate with a fitting strategy. The sampled posterior by the MCMC method is the product of a prior function and the likelihood function. While the user can choose the likelihood function, the prior function is a uniform distribution with customisable boundaries. Alongside optimisers and likelihood estimators, `fitting` includes a parameter space scanner (`fitting.explore_parameter_space`). This feature allows the exploration of the parameter space in a brute-force manner for the user to define the appropriate boundaries for the model fitting.

Several likelihood estimators are provided:

- the logarithm of the binomial distribution: $f(x,\theta) = \frac{n!}{x_1!\cdots x_k!} p_1(\theta)^{x_1}\cdots p_k(\theta)^{x_k}$, with n the total number of elements in the sequence, x_k and p_k are respectively the number of elements and the probability of an element to fall into in the k-th bin, and θ is the vector of parameters;
- the sum of the weighted squared residuals: $f(\theta) = \sum_k \frac{(d_k - p_k)^2}{\sigma_k^2}$, with d_k the measured histogram, p_k the model of the histogram, σ_k is the standard deviation of d_k and θ is the vector of parameters;
- the Pearson's χ^2 Pearson [1900]: $\chi^2 = \sum_k \frac{(d_k - N p_k(\theta))^2}{N p_k(\theta)}$, with d_k the measured histogram, p_k the model of the histogram at the k-th bin, N the number of events filling the histogram and θ is the vector of parameters.

Some of the nullers are already implemented in `instrument_models` such as GLINT Martinod et al. [2021] or LBTI Hinz et al. [2016], Ertel et al. [2020].

Functions in `histogram_tools` create histograms from measured data or simulations, perform random values generation and deliver diagnostic data to help to assess the reliability of the fit. The module `plots` includes functions to display the results of the fit, the parameter space as well as the diagnostic data. The module `load_files` includes functions to read HDF5 and FITS files; the user specifies the keywords to read, and the functions return a dictionary with the requested data. These can be then preprocessed with the tools, such as frame binning, sorting, slicing, and extracting spectral or photometric information, present in the `preprocessing` module.

4 Study cases of GRIP with real data

`GRIP` has been successfully used to measured null depth on already-published data from two instruments: GLINT and the LBTI nuller, with different features (Tab. 2). This library has successfully processed data on Arcturus Martinod et al. [2021] taken with GLINT and on β Leo Defrère et al. [2016] taken with the LBTI. For both, the same parameters were retrieved: the astrophysical null depth, and the average and standard deviation of a normal distribution modelling the phase fluctuations. `GRIP` used the same models found in their respective articles. The cases of study are conducted on two strategies implemented in `GRIP`: the MLE and the MCMC.

Table 2: Main features of GLINT and LBTI nullers

Features	GLINT	LBTI
Spectral band	1.5 ± 0.5 μm	$11 \pm$ 2.6μm
Spectral resolution	160	Broadband
Combiner platform	Integrated-optics	Bulk optics
AO correction	Yes	Yes
Fringe tracking	No	Yes
Acquisition of photometry, constructive and destructive interferences	Simultaneous	Sequential
Limiting noises	Phase fluctuations and camera read-out	Phase fluctuations and thermal background

4.1 Self-calibration with Maximum Likelihood Estimators

For the GLINT case, `GRIP` uses the same cost function and fitting strategy used in Martinod et al. [2021], namely the sum of the squared residuals and `scipy.optimize.least_squares`. For the LBTI case, `GRIP` uses a different estimator of the binomial mass probability function from the LBTI reduction code and a different fitting strategy than what was used in Defrère et al. [2016]. The cost function comes from the widely-used package `scipy` whereas LBTI reduction code uses an internally-developed estimator. The fitting strategy used in `GRIP` relies on the `minimize` method of `scipy` while the LBTI code performs a grid search. Both fits are performed on null depths calculated from fluxes of the destructive interference recorded in the camera (Fig. 3).

4.2 Self-calibration with MCMC

`GRIP` offers the possibility to perform MCMC with the `emcee` package. The main advantage of using this technique over MLE is having a more representative estimation of the posterior of the parameters, at the expense of a longer process if the walkers are not initialised near the optimal solutions, compared to MLE methods. For both GLINT and LBTI study cases, the fitted parameters are consistent with the ones found with the MLE techniques (FIgure 4).

4.3 Measuring the LBTI nuller transfer function

While the GLINT instrument model directly provides self-calibrated null depth, the model of the LBTI is not accurate enough and a calibration process is needed. Following the procedure detailed by Defrère et al. [2016], we have reduced the full dataset, made of one science target (β Leo) and three calibrators (HD 104979, HD 109742 and HD 108381) and calculated the transfer function of the instrument. These steps have been performed with the outputs from `GRIP` with the MLE and MCMC methods, and compared with the one published by Defrère et al. [2016] (Fig. 5). The transfer functions obtained from the MLE results is 0.147 ± 0.028 % and 0.161 ± 0.034 % from the MCMC results. Both transfer function are consistent with each other while

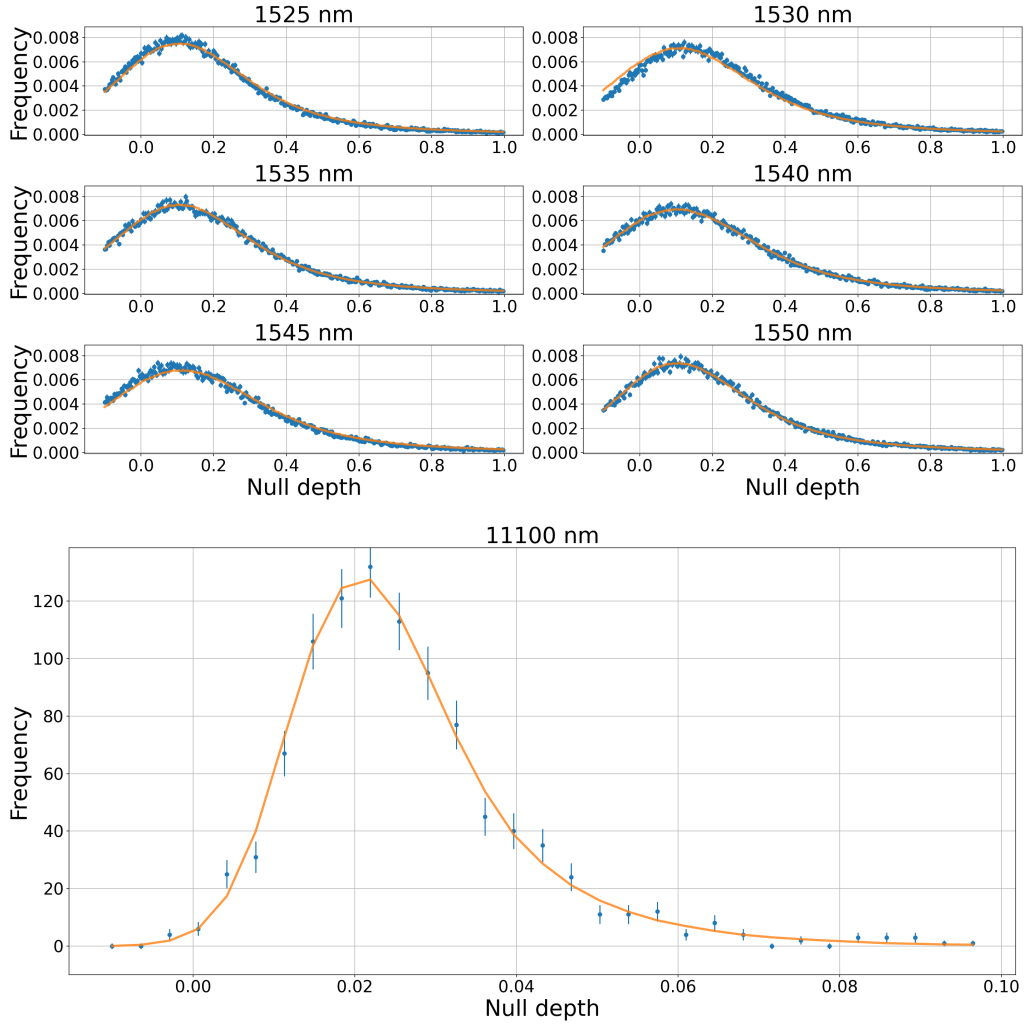

Figure 3: Fitted histograms of GLINT (top) and LBTI (bottom) data with `GRIP`. Top: GLINT data are Arcturus, taken with a baseline of 5.55 meters. The histograms of the null depth is made for every spectral channel are fitted at once. The fitted values are: $N_a = 0.0705 \pm 0.000137$, $\mu_{OPD} = 302 \pm 7.34$ nm and $\sigma_{OPD} = 163 \pm 0.378$ nm. Bottom: LBTI data are one observing block of β Leo, taken with a nominal baseline of 14.4 meters centre to centre, there is no spectral dispersion. The fitted values are: $N_a = 0.00714 \pm 0.00056$, $\mu_{OPD} = 174 \pm 11.4$ nm and $\sigma_{OPD} = 286 \pm 1.01$ nm. Unlike for GLINT data (left), the fitted null depth on this LBTI data set needs a calibration process with a reference star as the instrument simulator does not capture all the instrumental noise biases.

being higher than the published one. A bias remain between `GRIP`'s transfer functions and the published one ($0.057 \pm 0.025\%$), that appears to be systematics, with little incidence on the calibration of the null depths of the science star (see Section 4.4). These results confirm the LBTI nulling accuracy on the transfer function of a few 10^{-4}, required for the exozodiacal disk survey of the LBTI Ertel et al. [2018, 2020].

4.4 Comparison of the methods with the published results

We compare the calibrated null depths for both GLINT and LBTI cases with their published values. Self-calibrated null depths from `GRIP` are completely consistent with the published values for GLINT and LBTI (Figure 6). The null depths given by the package with the least squares method provide the same angular diameter of Arcturus on GLINT data. For the LBTI case, the null depths measured on β Leo, with the MLE and MCMC strategies, are calibrated by the transfer functions from the previous section. The calibrated null depths on β Leo obtained with `GRIP` with the MLE and MCMC methods are consistent with the published

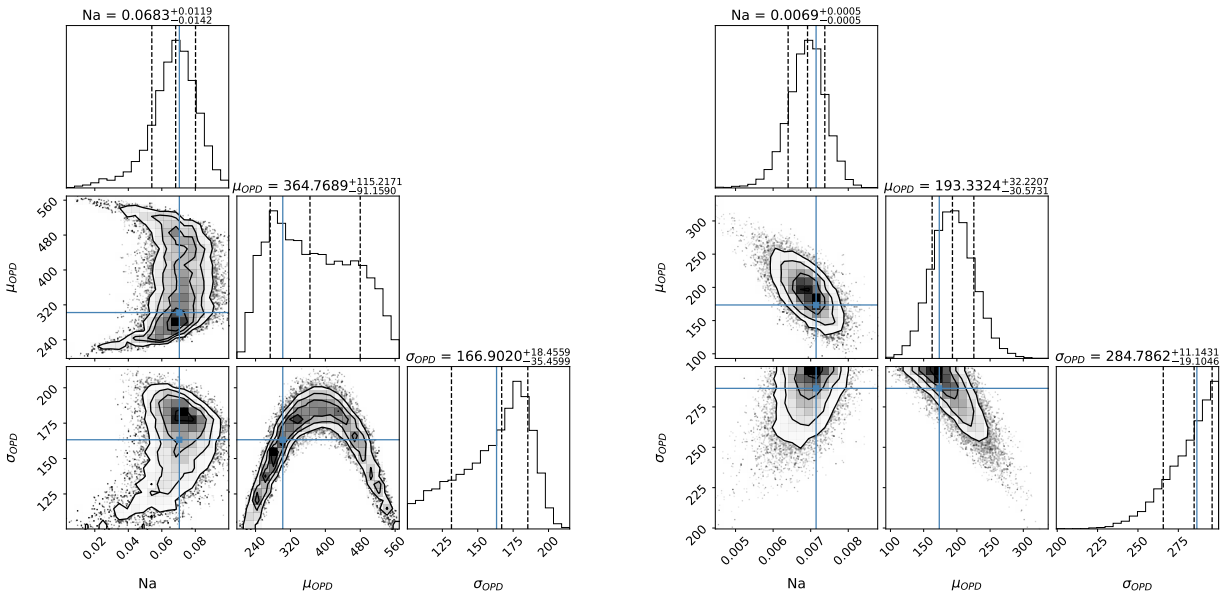

Figure 4: Corner plots of the inferred parameters of GLINT (left) and LBTI (right) data. The inferred parameters are the null depth Na, the location μ_{OPD} and scale σ_{OPD} parameters of the normal distribution describing the phase fluctuations, in nanometre. The blue lines represent the fitted values found with MLE method and use as the starting point for the MCMC algorithm. The values summarising the posterior distributions are the median, the 16-th and 84-th quantiles and are display on the top of each column of the corner plot. Left: same GLINT data as on the figure 3. Right: same LBTI data as on the figure 3.

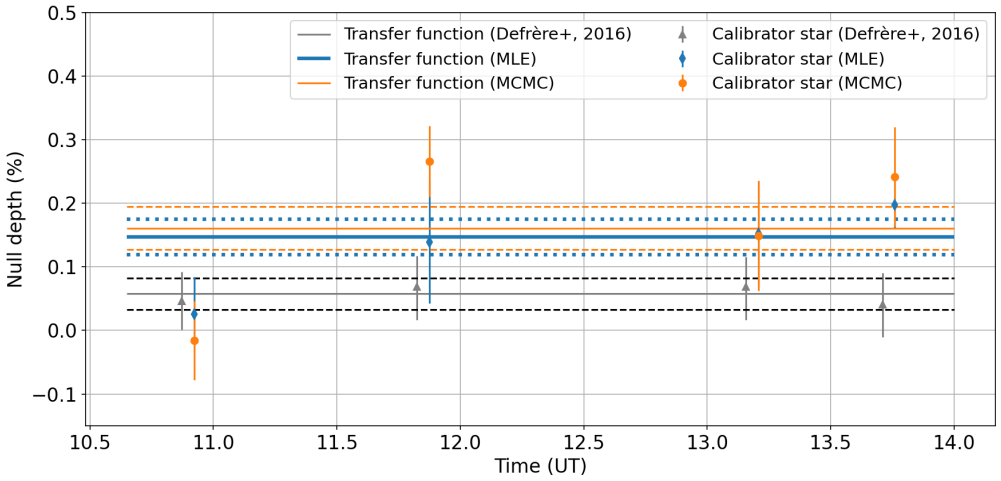

Figure 5: Transfer functions of the LBTI obtained with `GRIP` with the MLE and MCMC methods. They are compared to the published one Defrère et al. [2016].

values. Inddeed, the average null depth from the two β Leo points Defrère et al. [2016] is 0.52 ± 0.013 % and 0.52 ± 0.07 % from `GRIP` (the uncertainty is derived from the square root of the sum of the variances of each point).

5 Conclusion

`GRIP` is an open-source package providing methods to reduce data from any nuller according to the null self-calibration method. This versatility is possible by providing a simulator of the of the instrumental perturbation

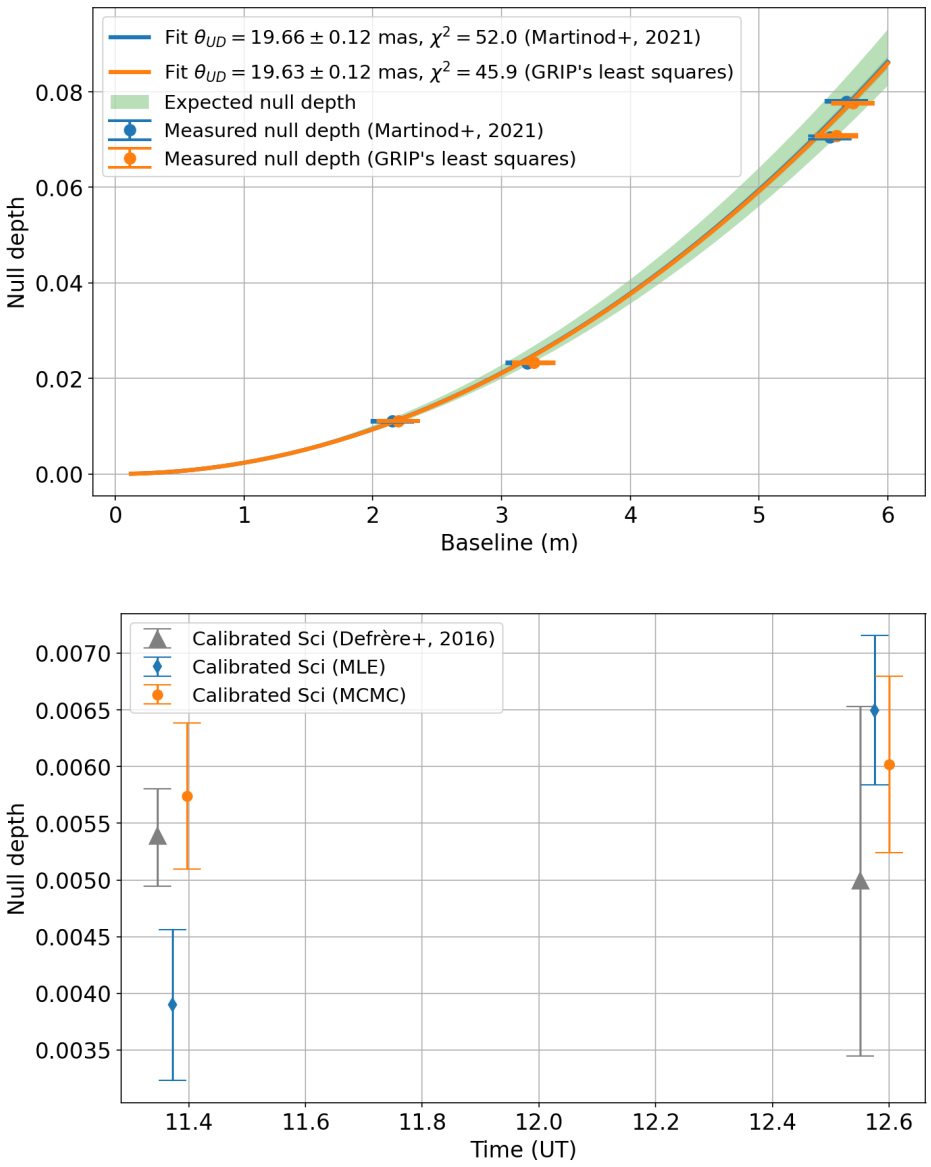

Figure 6: Comparison of the results obtained with GRIP for the published data on GLINT (top) and LBTI (bottom) data. On each figure, the data points from `GRIP` are artificially horizontally shifted to clarify the plots.

on the observables along with the data, then using `GRIP` features to exploit these inputs. This framework provides the basis for a standardised way of reducing nulling data, from nullers with different architectures or spectral coverage. It has been proven to provide reliable results through several optimisation strategies and to be compatible with any kind of nuller. `GRIP` is a scalable solution to implement new data reduction techniques, including neural network-based techniques or hierarchical Bayesian modelling. The results presented in this paper are consistent with previously published results and confirm interferometric nulling accuracy down to a few 10^{-4}. Future work will focus on pushing the nulling accuracy by implementing neural network-based techniques in `GRIP` and investigate its capabilities for stellar interferometers.

Besides, while `GRIP` adresses the question of reducing the data through the NSC approach to provide estimates of the null depth, it does not include their interpretation. This should be addressed in the future through the NIFITS standard, which will mirror the usage of OIFITS as a medium for astrophysical interpretation of the data. This format and the interface with `GRIP` is under investigation.

Acknowledgments

M-A.M. has received funding from the European Union's Horizon 2020 research and innovation programme under grant agreement No. 101004719.

D.D., G.G., and M-A.M. acknowledge support from the European Research Council (ERC) under the European Union's Horizon 2020 research and innovation program (grant agreement No. CoG - 866070).

R.L. has received funding from the Research Foundation - Flanders (FWO) under the grant number 1234224N.

SE is supported by the National Aeronautics and Space Administration through the Astrophysics Decadal Survey Precursor Science program (Grant No. 80NSSC23K1473).

Data Availability

The data produced in this study are available from the corresponding author on reasonable request.

References

R. N. Bracewell. Detecting nonsolar planets by spinning infrared interferometer. Nature, 274(5673):780–781, August 1978. doi: 10.1038/274780a0.

Valentin Christiaens, Carlos Gonzalez, Ralf Farkas, Carl-Henrik Dahlqvist, Evert Nasedkin, Julien Milli, Olivier Absil, Henry Ngo, Carles Cantero, Alan Rainot, Iain Hammond, Markus Bonse, Faustine Cantalloube, Arthur Vigan, Vijay Kompella, and Paul Hancock. VIP: A Python package for high-contrast imaging. *The Journal of Open Source Software*, 8(81):4774, January 2023a. doi: 10.21105/joss.04774.

Valentin Christiaens, Iain Hammond, Sandrine Juillard, Elena Kokoulina, and Olga Balsalobre-Ruza. VCAL-SPHERE: Hybrid pipeline for reduction of VLT/SPHERE data. Astrophysics Source Code Library, record ascl:2311.002, November 2023b.

Valentin Christiaens, Matthias Samland, Danny Gasman, Milou Temmink, and Giulia Perotti. MINDS: Hybrid pipeline for the reduction of JWST/MIRI-MRS data. Astrophysics Source Code Library, record ascl:2403.007, March 2024.

Kyle Cranmer, Johann Brehmer, and Gilles Louppe. The frontier of simulation-based inference. *Proceedings of the National Academy of Science*, 117(48):30055–30062, December 2020. doi: 10.1073/pnas.1912789117.

D. Defrère, P. M. Hinz, A. J. Skemer, G. M. Kennedy, V. P. Bailey, W. F. Hoffmann, B. Mennesson, R. Millan-Gabet, W. C. Danchi, O. Absil, P. Arbo, C. Beichman, G. Brusa, G. Bryden, E. C. Downey, O. Durney, S. Esposito, A. Gaspar, P. Grenz, C. Haniff, J. M. Hill, J. Lebreton, J. M. Leisenring, J. R. Males, L. Marion, T. J. McMahon, M. Montoya, K. M. Morzinski, E. Pinna, A. Puglisi, G. Rieke, A. Roberge, E. Serabyn, R. Sosa, K. Stapeldfeldt, K. Su, V. Vaitheeswaran, A. Vaz, A. J. Weinberger, and M. C. Wyatt. First-light LBT Nulling Interferometric Observations: Warm Exozodiacal Dust Resolved within a Few AU of η Crv. ApJ, 799(1):42, January 2015. doi: 10.1088/0004-637X/799/1/42.

D. Defrère, P. M. Hinz, B. Mennesson, W. F. Hoffmann, R. Millan-Gabet, A. J. Skemer, V. Bailey, W. C. Danchi, E. C. Downey, O. Durney, P. Grenz, J. M. Hill, T. J. McMahon, M. Montoya, E. Spalding, A. Vaz, O. Absil, P. Arbo, H. Bailey, G. Brusa, G. Bryden, S. Esposito, A. Gaspar, C. A. Haniff, G. M. Kennedy, J. M. Leisenring, L. Marion, M. Nowak, E. Pinna, K. Powell, A. Puglisi, G. Rieke, A. Roberge, E. Serabyn, R. Sosa, K. Stapeldfeldt, K. Su, A. J. Weinberger, and M. C. Wyatt. Nulling Data Reduction and On-sky Performance of the Large Binocular Telescope Interferometer. ApJ, 824(2):66, June 2016. doi: 10.3847/0004-637X/824/2/66.

D. Defrère, P. M. Hinz, G. M. Kennedy, J. Stone, J. Rigley, S. Ertel, A. Gaspar, V. P. Bailey, W. F. Hoffmann, B. Mennesson, R. Millan-Gabet, W. C. Danchi, O. Absil, P. Arbo, C. Beichman, M. Bonavita, G. Brusa, G. Bryden, E. C. Downey, S. Esposito, P. Grenz, C. Haniff, J. M. Hill, J. M. Leisenring, J. R. Males,

T. J. McMahon, M. Montoya, K. M. Morzinski, E. Pinna, A. Puglisi, G. Rieke, A. Roberge, H. Rousseau, E. Serabyn, E. Spalding, A. J. Skemer, K. Stapelfeldt, K. Su, A. Vaz, A. J. Weinberger, and M. C. Wyatt. The HOSTS Survey: Evidence for an Extended Dust Disk and Constraints on the Presence of Giant Planets in the Habitable Zone of β Leo. AJ, 161(4):186, April 2021. doi: 10.3847/1538-3881/abe3ff.

D. Defrère, O. Absil, J.-P. Berger, T. Boulet, W. C. Danchi, S. Ertel, A. Gallenne, F. Hénault, P. Hinz, E. Huby, M. Ireland, S. Kraus, L. Labadie, J.-B. Le Bouquin, G. Martin, A. Matter, A. Mérand, B. Mennesson, S. Minardi, J. D. Monnier, B. Norris, G. Orban de Xivry, E. Pedretti, J.-U. Pott, M. Reggiani, E. Serabyn, J. Surdej, K. R. W. Tristram, and J. Woillez. The path towards high-contrast imaging with the VLTI: the Hi-5 project. *Experimental Astronomy*, 46:475–495, December 2018a. ISSN 0922-6435. doi: 10.1007/s10686-018-9593-2. URL http://adsabs.harvard.edu/abs/2018ExA....46..475D.

D. Defrère, M. Ireland, O. Absil, J.-P. Berger, W. C. Danchi, S. Ertel, A. Gallenne, F. Hénault, P. Hinz, E. Huby, S. Kraus, L. Labadie, J.-B. Le Bouquin, G. Martin, A. Matter, B. Mennesson, A. Mérand, S. Minardi, J. D. Monnier, B. Norris, G. Orban de Xivry, E. Pedretti, J.-U. Pott, M. Reggiani, E. Serabyn, J. Surdej, K. R. W. Tristram, and J. Woillez. Hi-5: a potential high-contrast thermal near-infrared imager for the VLTI. In *Optical and Infrared Interferometry and Imaging VI*, volume 10701, pages 223–237. SPIE, July 2018b. doi: 10.1117/12.2313700. URL https://www.spiedigitallibrary.org/conference-proceedings-of-spie/10701/107010U/Hi-5--a-potential-high-contrast-thermal-near-infrared/10.1117/12.2313700.full.

Denis Defrère, Azzurra Bigioli, Colin Dandumont, Germain Garreau, Romain Laugier, Marc-Antoine Martinod, Olivier Absil, Jean-Philippe Berger, Emilie Bouzerand, Benjamin Courtney-Barrer, Alexandre Emsenhuber, Steve Ertel, Jonathan Gagne, Adrian Glauser, Simon Gross, Michael J. Ireland, Harry-Dean Kenchington, Jacques Kluska, Stefan Kraus, Lucas Labadie, Viktor Laborde, Alain Léger, Jarron Leisenring, Jérôme Loicq, Guillermo Martin, Johan Morren, Alexis Matter, Alexandra Mazzoli, Kwinten Missiaen, Salman Muhammad, Marc Ollivier, Gert Raskin, Hélène Rousseau, Ahmed Sanny, Simon Verlinden, Bart Vandenbussche, and Julien Woillez. L-band nulling interferometry at the VLTI with Asgard/Hi-5: status and plans. In *Optical and Infrared Interferometry and Imaging VIII*, volume 12183, pages 184–199. SPIE, August 2022. doi: 10.1117/12.2627953. URL https://www.spiedigitallibrary.org/conference-proceedings-of-spie/12183/121830H/L-band-nulling-interferometry-at-the-VLTI-with-Asgard-Hi/10.1117/12.2627953.full.

S. Ertel, D. Defrère, P. Hinz, B. Mennesson, G. M. Kennedy, W. C. Danchi, C. Gelino, J. M. Hill, W. F. Hoffmann, G. Rieke, A. Shannon, E. Spalding, J. M. Stone, A. Vaz, A. J. Weinberger, P. Willems, O. Absil, P. Arbo, V. P. Bailey, C. Beichman, G. Bryden, E. C. Downey, O. Durney, S. Esposito, A. Gaspar, P. Grenz, C. A. Haniff, J. M. Leisenring, L. Marion, T. J. McMahon, R. Millan-Gabet, M. Montoya, K. M. Morzinski, E. Pinna, J. Power, A. Puglisi, A. Roberge, E. Serabyn, A. J. Skemer, K. Stapelfeldt, K. Y. L. Su, V. Vaitheeswaran, and M. C. Wyatt. The HOSTS Survey—Exozodiacal Dust Measurements for 30 Stars. AJ, 155(5):194, May 2018. doi: 10.3847/1538-3881/aab717.

S. Ertel, D. Defrère, P. Hinz, B. Mennesson, G. M. Kennedy, W. C. Danchi, C. Gelino, J. M. Hill, W. F. Hoffmann, J. Mazoyer, G. Rieke, A. Shannon, K. Stapelfeldt, E. Spalding, J. M. Stone, A. Vaz, A. J. Weinberger, P. Willems, O. Absil, P. Arbo, V. P. Bailey, C. Beichman, G. Bryden, E. C. Downey, O. Durney, S. Esposito, A. Gaspar, P. Grenz, C. A. Haniff, J. M. Leisenring, L. Marion, T. J. McMahon, R. Millan-Gabet, M. Montoya, K. M. Morzinski, S. Perera, E. Pinna, J. U. Pott, J. Power, A. Puglisi, A. Roberge, E. Serabyn, A. J. Skemer, K. Y. L. Su, V. Vaitheeswaran, and M. C. Wyatt. The HOSTS Survey for Exozodiacal Dust: Observational Results from the Complete Survey. AJ, 159(4):177, April 2020. doi: 10.3847/1538-3881/ab7817.

Daniel Foreman-Mackey, David W. Hogg, Dustin Lang, and Jonathan Goodman. emcee: The MCMC Hammer. PASP, 125(925):306, March 2013. doi: 10.1086/670067.

Carlos Alberto Gomez Gonzalez, Olivier Wertz, Olivier Absil, Valentin Christiaens, Denis Defrère, Dimitri Mawet, Julien Milli, Pierre-Antoine Absil, Marc Van Droogenbroeck, Faustine Cantalloube, Philip M. Hinz,

Andrew J. Skemer, Mikael Karlsson, and Jean Surdej. VIP: Vortex Image Processing Package for High-contrast Direct Imaging. AJ, 154(1):7, July 2017. doi: 10.3847/1538-3881/aa73d7.

C. Hanot, B. Mennesson, S. Martin, K. Liewer, F. Loya, D. Mawet, P. Riaud, O. Absil, and E. Serabyn. Improving Interferometric Null Depth Measurements using Statistical Distributions: Theory and First Results with the Palomar Fiber Nuller. ApJ, 729(2):110, March 2011. doi: 10.1088/0004-637X/729/2/110.

P. M. Hinz, D. Defrère, A. Skemer, V. Bailey, J. Stone, E. Spalding, A. Vaz, E. Pinna, A. Puglisi, S. Esposito, M. Montoya, E. Downey, J. Leisenring, O. Durney, W. Hoffmann, J. Hill, R. Millan-Gabet, B. Mennesson, W. Danchi, K. Morzinski, P. Grenz, M. Skrutskie, and S. Ertel. Overview of LBTI: a multipurpose facility for high spatial resolution observations. In Fabien Malbet, Michelle J. Creech-Eakman, and Peter G. Tuthill, editors, *Optical and Infrared Interferometry and Imaging V*, volume 9907 of *Society of Photo-Optical Instrumentation Engineers (SPIE) Conference Series*, page 990704, August 2016. doi: 10.1117/12.2233795.

Philip M. Hinz, J. Roger P. Angel, William F. Hoffmann, Donald W. McCarthy, Patrick C. McGuire, Matt Cheselka, Joseph L. Hora, and Neville J. Woolf. First results of nulling interferometry with the Multiple-Mirror Telescope. In Robert D. Reasenberg, editor, *Astronomical Interferometry*, volume 3350 of *Society of Photo-Optical Instrumentation Engineers (SPIE) Conference Series*, pages 439–447, July 1998. doi: 10.1117/12.317108.

Marc-Antoine Martinod, Barnaby Norris, Peter Tuthill, Tiphaine Lagadec, Nemanja Jovanovic, Nick Cvetojevic, Simon Gross, Alexander Arriola, Thomas Gretzinger, Michael J. Withford, Olivier Guyon, Julien Lozi, Sébastien Vievard, Vincent Deo, Jon S. Lawrence, and Sergio Leon-Saval. Scalable photonic-based nulling interferometry with the dispersed multi-baseline GLINT instrument. *Nature Communications*, 12: 2465, January 2021. doi: 10.1038/s41467-021-22769-x.

Marc-Antoine Martinod, Denis Defrère, Romain Laugier, Steve Ertel, Olivier Absil, Barnaby Norris, Germain Garreau, and Bertrand Mennesson. Generic data reduction for nulling interferometry package: the grip of a single data reduction package on all the nulling interferometers. In Jens Kammerer, Stephanie Sallum, and Joel Sanchez-Bermudez, editors, *Optical and Infrared Interferometry and Imaging IX*, volume 13095, page 130951A. International Society for Optics and Photonics, SPIE, 2024. doi: 10.1117/12.3017506. URL https://doi.org/10.1117/12.3017506.

B. Mennesson, C. Hanot, E. Serabyn, K. Liewer, S. R. Martin, and D. Mawet. High-contrast Stellar Observations within the Diffraction Limit at the Palomar Hale Telescope. ApJ, 743(2):178, December 2011. doi: 10.1088/0004-637X/743/2/178.

Bertrand Mennesson, Denis Defrère, Matthias Nowak, Philip Hinz, Rafael Millan-Gabet, Olivier Absil, Vanessa Bailey, Geoffrey Bryden, William Danchi, Grant M. Kennedy, Lindsay Marion, Aki Roberge, Eugene Serabyn, Andy J. Skemer, Karl Stapelfeldt, Alycia J. Weinberger, and Mark Wyatt. Making high-accuracy null depth measurements for the LBTI exozodi survey. In Fabien Malbet, Michelle J. Creech-Eakman, and Peter G. Tuthill, editors, *Optical and Infrared Interferometry and Imaging V*, volume 9907 of *Society of Photo-Optical Instrumentation Engineers (SPIE) Conference Series*, page 99070X, August 2016. doi: 10.1117/12.2231839.

Barnaby R. M. Norris, Nick Cvetojevic, Tiphaine Lagadec, Nemanja Jovanovic, Simon Gross, Alexander Arriola, Thomas Gretzinger, Marc-Antoine Martinod, Olivier Guyon, Julien Lozi, Michael J. Withford, Jon S. Lawrence, and Peter Tuthill. First on-sky demonstration of an integrated-photonic nulling interferometer: the GLINT instrument. MNRAS, 491(3):4180–4193, January 2020. doi: 10.1093/mnras/stz3277.

Ryosuke Okuta, Yuya Unno, Daisuke Nishino, Shohei Hido, and Crissman Loomis. Cupy: A numpy-compatible library for nvidia gpu calculations. In *Proceedings of Workshop on Machine Learning Systems (LearningSys) in The Thirty-first Annual Conference on Neural Information Processing Systems (NIPS)*, 2017. URL http://learningsys.org/nips17/assets/papers/paper_16.pdf.

Karl Pearson. X. on the criterion that a given system of deviations from the probable in the case of a correlated system of variables is such that it can be reasonably supposed to have arisen from random sampling. *The*

London, Edinburgh, and Dublin Philosophical Magazine and Journal of Science, 50(302):157–175, 1900. doi: 10.1080/14786440009463897. URL https://doi.org/10.1080/14786440009463897.

S. P. Quanz, M. Ottiger, E. Fontanet, J. Kammerer, F. Menti, F. Dannert, A. Gheorghe, O. Absil, V. S. Airapetian, E. Alei, R. Allart, D. Angerhausen, S. Blumenthal, L. A. Buchhave, J. Cabrera, Ó. Carrión-González, G. Chauvin, W. C. Danchi, C. Dandumont, D. Defrére, C. Dorn, D. Ehrenreich, S. Ertel, M. Fridlund, A. García Muñoz, C. Gascón, J. H. Girard, A. Glauser, J. L. Grenfell, G. Guidi, J. Hagelberg, R. Helled, M. J. Ireland, M. Janson, R. K. Kopparapu, J. Korth, T. Kozakis, S. Kraus, A. Léger, L. Leedjärv, T. Lichtenberg, J. Lillo-Box, H. Linz, R. Liseau, J. Loicq, V. Mahendra, F. Malbet, J. Mathew, B. Mennesson, M. R. Meyer, L. Mishra, K. Molaverdikhani, L. Noack, A. V. Oza, E. Pallé, H. Parviainen, A. Quirrenbach, H. Rauer, I. Ribas, M. Rice, A. Romagnolo, S. Rugheimer, E. W. Schwieterman, E. Serabyn, S. Sharma, K. G. Stassun, J. Szulágyi, H. S. Wang, F. Wunderlich, M. C. Wyatt, and LIFE Collaboration. Large Interferometer For Exoplanets (LIFE). I. Improved exoplanet detection yield estimates for a large mid-infrared space-interferometer mission. A&A, 664:A21, August 2022. doi: 10.1051/0004-6361/202140366.

Sascha P. Quanz, Jens Kammerer, Denis Defrère, Olivier Absil, Adrian M. Glauser, and Daniel Kitzmann. Exoplanet science with a space-based mid-infrared nulling interferometer. In Michelle J. Creech-Eakman, Peter G. Tuthill, and Antoine Mérand, editors, *SPIE*, volume 10701 of *Society of Photo-Optical Instrumentation Engineers (SPIE) Conference Series*, page 107011I, July 2018. doi: 10.1117/12.2312051.

E. Serabyn, B. Mennesson, S. Martin, K. Liewer, and J. Kühn. Nulling at short wavelengths: theoretical performance constraints and a demonstration of faint companion detection inside the diffraction limit with a rotating-baseline interferometer. MNRAS, 489(1):1291–1303, October 2019. doi: 10.1093/mnras/stz2163.